Reactive Oxygen Species from Mitochondria Induce Cyclooxygenase-2 Gene Expression in Human Mesangial Cells

Potential Role in Diabetic Nephropathy

Shinsuke Kiritoshi,[1] Takeshi Nishikawa,[1] Kazuhiro Sonoda,[1] Daisuke Kukidome,[1] Takahumi Senokuchi,[1] Tomoko Matsuo,[1] Takeshi Matsumura,[1] Hiroshi Tokunaga,[1] Michael Brownlee,[2] and Eiichi Araki[1]

Hyperglycemia increases the production of reactive oxygen species (ROS) from the mitochondrial electron transport chain in bovine endothelial cells. Because several studies have postulated a role for prostaglandins (PGs) in the glomerular hyperfiltration seen in early diabetes, we evaluated the effect of mitochondrial ROS on expression of the inducible isoform of cyclooxygenase (COX-2) in cultured human mesangial cells (HMCs). We first confirmed that incubation of HMC with 30 mmol/l glucose significantly increased COX-2 mRNA but not COX-1 mRNA, compared with 5.6 mmol/l glucose. Similarly, incubation of HMCs with 30 mmol/l glucose significantly increased mitochondrial membrane potential, intracellular ROS production, COX-2 protein expression, and PGE$_2$ synthesis, and these events were completely suppressed by thenoyltrifluoroacetone or carbonyl cyanide m-chlorophenylhydrazone, inhibitors of mitochondrial metabolism, or by overexpression of uncoupling protein-1 or manganese superoxide dismutase. Furthermore, increased expression of COX-2 mRNA and protein was confirmed in glomeruli of streptozotocin-induced diabetic mice. In addition, hyperglycemia induced activation of the COX-2 gene promoter, which was completely abrogated by mutation of two nuclear factor κB (NF-κB) binding sites in the promoter region. Our results suggest that hyperglycemia increases mitochondrial ROS production, resulting in NF-κB activation, COX-2 mRNA induction, COX-2 protein production, and PGE$_2$ synthesis. This chain of events might contribute to the pathogenesis of diabetic nephropathy. *Diabetes* 52:2570–2577, 2003

Increased oxidative stress is considered to be one of the common pathogenic factors in diabetic complications (1). Recently, we showed that hyperglycemia-induced production of reactive oxygen species (ROS) is abrogated by inhibitors of mitochondrial metabolism or by overexpression of uncoupling protein-1 (UCP-1) or manganese superoxide dismutase (MnSOD) (2). Normalization of mitochondrial ROS production by each of these agents prevents glucose-induced activation of protein kinase C, formation of advanced glycation end products, accumulation of sorbitol, and activation of nuclear factor κB (NF-κB) in bovine vascular endothelial cells, all of which are known to be involved in the development of diabetic complications (2). However, it remains unclear how ROS from the mitochondrial electron transport chain could contribute to the progression of diabetic microvascular complications, including nephropathy, retinopathy, and neuropathy.

Glomerular hyperfiltration is a characteristic finding of early diabetes in both humans and animal models of diabetes and may play a major role in the pathogenesis of diabetic nephropathy (3,4). The mechanisms that mediate an increase in glomerular filtration rate are not well identified, but the vascular reactivity of the renal glomerular efferent arterioles has been shown to be controlled, at least in part, by the release of endogenously synthesized prostaglandins (PGs), allowing autoregulation of glomerular capillary pressure (5). Because PGs play a role in controlling renal function, it has been proposed that changes in PG production may contribute to the hemodynamic changes observed in diabetes. Several studies have shown that renal PG production is increased at the onset of diabetes (6,7).

Cyclooxygenase (COX), also known as PGH synthase, is a membrane-bound, bifunctional enzyme that catalyzes the conversion of arachidonic acid to PGG$_2$ by its cyclooxygenase activity, and of PGG$_2$ to PGH$_2$ by peroxidase activity. It is the rate-limiting step in biosynthesis of the biologically active and physiologically important PGs (8). Recently, two isoforms of COX were identified, COX-1 and COX-2 (9). COX-1 is constitutively expressed in most tissues. In contrast, COX-2 operates as an inducible en-

zyme with low or undetectable levels in most tissues, and its expression can be markedly increased by a number of inflammatory cytokines, mitogenic factors, and physical stimuli (10,11). The COX-2 gene contains putative binding motifs for NF-κB (12). Recent evidence has suggested that PGs synthesized by COX-2 play a role in physiological regulation in the normal kidney, being involved in modulation of afferent arteriolar vasoconstriction after stimulation of tubuloglomerular feedback (13). Therefore, we hypothesized that hyperglycemia-induced ROS production through the mitochondrial electron transport chain could increase the expression of the COX-2 gene and play an important role in diabetes-induced renal hemodynamic alterations.

The present study was designed to determine the expression of COX-2 gene and production of ROS induced by hyperglycemia in cultured human mesangial cells (HMCs). To elucidate the role of mitochondrial ROS on expression of the COX-2 gene and PGE$_2$ synthesis, we investigated the effects of inhibitors of mitochondrial metabolism and overexpression of either UCP-1 or MnSOD. In addition, to clarify further the mechanisms of hyperglycemia-induced COX-2 expression, we performed reporter gene transfection assays using wild-type/mutant constructs of the COX-2 gene promoter.

RESEARCH DESIGN AND METHODS

Cells and culture. HMCs were obtained from BioWhittaker (Walkersville, MD) and cultured in Dulbecco's modified Eagle's medium (DMEM; GIBCO BRL, Grand Island, NY) containing 10 mmol/l HEPES, 20% FCS, 100 units/ml penicillin, and 100 μg/ml streptomycin in a humidified air/5% CO$_2$ atmosphere at 37°C (14). All cells were studied at passage 4–6. Near-confluent HMCs were incubated with DMEM containing 5% FCS for 48 h to arrest and synchronize cell growth. After this period, the medium was changed to fresh DMEM (5% FCS) containing either 5.6 or 30 mmol/l glucose. Cells were also incubated with 30 mmol/l glucose medium in the presence of an inhibitor of electron transport complex II, 10 μmol/l thenoyltrifluoroacetone (TTFA; Sigma, St. Louis, MO), an uncoupler, 0.5 μmol/l carbonyl cyanide *m*-chlorophenylhydrazone (CCCP; Sigma), or a relatively specific inhibitor of COX-2, 10 μmol/l meloxicam (Calbiochem, San Diego, CA), or they were infected with UCP-1 adenovirus or MnSOD adenovirus, as described below. During this experiment, the cell viability, as evaluated by alamarBlue assay (Dainippon Pharmaceutical, Osaka, Japan), did not change (data not shown).

Adenoviral vectors. Adenoviral vectors were prepared as described previously (15). Rat UCP-1 sense and antisense cDNAs were provided by Dr. D. Riguier (Center National de la Recherche Scientifique-Unite Propre 1511, Meudon, France), and human MnSOD cDNA was provided by Dr. L. Oberley (University of Iowa College of Medicine, Iowa City, IA). The cDNAs were cloned into the shuttle vector pAd5CMVK-NpA, and adenoviral vectors were prepared by the Gene Transfer Vector Core at the University of Iowa.

RNA isolation and quantitative RT-PCR analysis of COX-1 and COX-2 expression. After incubation for 24 h in each condition, total cellular RNA was isolated from cells using Trizol reagent according to the protocol (Life Technologies, Gaithersburg, MD). For quantifying COX-1 and COX-2 transcripts, the LightCycler System (Roche Molecular Biochemicals, Indianapolis, IN) was used (16). PCRs were performed using SYBR Green I master mix and specific primers for human COX-1: 5′-AGAAACAACAGGGGAAACTA-3′ and 5′-AAGAAAGGACAGGACACAAG-3′; human COX-2: 5′-AAGTCCCTGAGCATC TACGGTTT-3′ and 5′-GTTGTGTTCCCTCAGCCAGATT-3′; mouse COX-2: 5′-CACAGCCTACCAAAACAGCCA-3′ and 5′-GCTCAGTTGAACGCCTTTTGA-3′; and human β-actin primers: 5′-TCACCCACACTGTGCCCATCTACGA-3′ and 5′-CAGCGGAACCGCTCATTGCCAATGG-3′. Mouse β-actin primers were purchased from Promega (Madison, WI). To assess the specificity of the amplified PCR products, after the last cycle, we performed a melting curve analysis and subjected reaction end products to electrophoresis in 2% agarose gels, and we compared band intensities by imaging of ethidium bromide–stained gels.

Creation of diabetic mice and isolation of glomeruli. Diabetes was induced in 6-week-old ddy male mice by two consecutive intraperitoneal injections of streptozotocin (100 mg · kg^{-1} · d^{-1}; Sigma) dissolved in 10 mmol/l Na citrate, pH 5.5. Nondiabetic mice received an injection of buffer alone.

Once glycosuria was detected, regular insulin (0.1–0.2 units) was administered subcutaneously every day to prevent ketonuria and maintain a moderately elevated blood glucose concentration (22–28 mmol/l). Streptozotocin-induced diabetic mice and age-matched control mice were anesthetized after 1 week, and glomeruli were isolated by using Dynabeads (Dynal, Oslo, Norway) as described (17). Briefly, mice were perfused with 8×10^7 Dynabeads diluted in 40 ml of PBS through the heart. The kidneys were removed, minced, and digested in collagenase at 37°C for 15 min. The collagenase-digested tissue was gently pressed through a 100-μm cell strainer (BD Biosciences, Stockholm, Sweden). Finally, glomeruli were gathered by a magnetic particle concentrator (Dynal). During the procedure, kidney tissues were kept at 4°C except for digestion with collagenase.

Fluorescence and light microscopy. HMCs were incubated with DMEM containing 1 μmol/l RedoxSensor Red CC-1 (Molecular Probes Europe BV, Leiden, the Netherlands) at 37°C for 10 min and were coincubated with 0.1 μmol/l MitoTracker Green FM (Molecular Probes), a fluorescent stain for mitochondria, for 30 min, after incubation for 3 h with 5.6 or 30 mmol/l glucose. A confocal laser-scanning microscope (model FV500; Olympus, Tokyo, Japan) was equipped for epifluorescent illumination.

Measurement of intracellular ROS. The intracellular formation of ROS was detected using the probe 6-carboxy-2′,7′-dichlorodihydrofluorescein diacetate, di(acetoxymethyl ester) (H$_2$DCF-DA) (C-2938; Molecular Probes) after HMCs were incubated for 3 h under each condition as described (2,18). ROS concentrations were determined from a standard curve of H$_2$O$_2$ (5–100 μmol/l) and were expressed as a percentage of ROS incubated in 5.6 mmol/l glucose.

Western blot analysis of COX-2 protein. Western blot analysis was performed in HMCs treated under each condition for 24 h or in glomeruli isolated from diabetic mice or nondiabetic control mice. Cells or glomeruli were lysed in buffer (50 mmol/l HEPES, 150 mmol/l NaCl, 1% Triton X-100, 5 mmol/l EDTA, 5 mmol/l EGTA, 20 mmol/l Na$_4$P$_2$O$_7$-10 H$_2$O, 1 mmol/l Na$_3$VO$_4$, 20 mmol/l NaF, and 10 μmol/l PMSF) and then sonicated at 4°C. Homogenates were centrifuged at 20,000g for 20 min at 4°C, and supernatant was collected. Samples were denatured in SDS-PAGE sample buffer for 5 min at 97°C, separated through an SDS-polyacrylamide (10%) gel, and transferred to a nitrocellulose membrane. Membranes were washed with Tris-buffered saline (TBS-T; 10 mmol/l Tris, 150 mmol/l NaCl, and 0.05% Tween-20), blocked for 1 h with TBS-T containing 5% nonfat dry milk, and incubated for 2 h with rabbit polyclonal anti-human COX-2 antiserum (IBL, Gunma, Japan) or rabbit polyclonal anti-murine COX-2 antiserum (Cayman Chemical, Ellsworth, MI) in TBS-T. Immunodetection was accomplished by incubating membranes with a goat anti-rabbit IgG-horseradish peroxidase and secondary antibody in TBS-T containing 5% nonfat dry milk for 30 min. Visualization was performed with a BM Chemiluminescence Blotting Substrate kit (Roche Diagnostics, Mannheim, Germany) according to the instructions provided by the manufacturer.

Measurement of PGE$_2$. Medium (50 μl) was collected from the HMC culture dish under each condition after incubation for 24 h and was assayed directly. The concentration of PGE$_2$ in culture medium was measured in 96-well reaction plates using an enzyme immunosorbent assay kit (Cayman Chemical) using the protocol. The amounts of PGE$_2$ in medium were corrected by the total amount of protein in the corresponding cell extracts.

Transient transfection and luciferase assay. HMCs were transfected by a liposome-mediated method using Lipofectamine 2000 reagent (LP2000; Invitrogen, San Diego, CA). A 550-bp PCR fragment from the 5′-upstream region (from bases −497 to 32) of the human COX-2 gene was subcloned between the *Nhe*I and *Hin*dIII sites of pGL-3 basic (Promega), a luciferase reporter plasmid (pGL3-pCOX2). There are two consensus sequences for the NF-κB binding site in the COX-2 promoter region: the NF-κB–5′ site (5′-GGAGAGGGGATTCCC TGCGCC-3′, within −452 to −442 from the transcriptional start site) (19) and the NF-κB–3′ site (5′-AGAGTGGGGACTACCCCCTCT-3′, −228 to −208). The mutated COX-2 promoter-luciferase reporters were generated from pGL3-pCOX2, introducing the mutation using PCR mutagenesis. As described previously (20), the NF-κB–5′ and NF-κB–3′ sites were mutated from 5′-GGAGAGGGGATTCCCTGCGCC-3′ to 5′-GGAGAGGCCATTCCCTGCGCC-3′ (NF mut1), and 5′-AGAGTGGGGACTACCCCCTCT-3′ to 5′-AGAGTGGCCAC TACCCCCTCT-3′ (NF mut2), respectively. HMCs were cotransfected with pGL3-pCOX2 and pGL3-pSV40 vector containing the Renilla luciferase gene (Promega). The latter was used as an internal control to monitor transfection efficiency at a 1:1 pGL3-pCOX2/pGL3-pSV40 ratio. A transfection mixture containing a 2 μg DNA/5 μl LP2000 ratio was added for 4 h in the absence of serum. After removal of transfection medium, cells were treated with the corresponding reagents for 48 h. The Dual-Luciferase Reporter Assay System (Promega) was used to determine luciferase activity. Firefly luciferase activity was normalized for variations in transfection efficiency as determined by the Renilla luciferase activity measurements. Transfections were performed in triplicate wells, and each experiment was repeated twice.
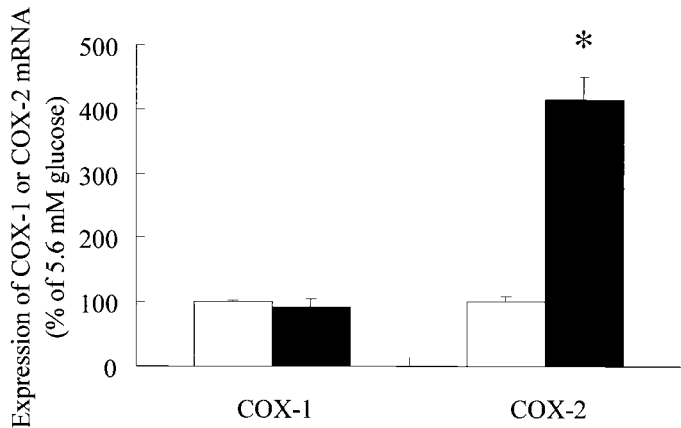
FIG. 1. Effect of high glucose on expression of COX-1 and COX-2 mRNAs in HMCs. Cells were incubated for 24 h with 5.6 mmol/l glucose (□) or 30 mmol/l glucose (■). Total RNA was isolated, and COX-1 and COX-2 mRNAs were quantified by a real-time RT-PCR method. Results are expressed as values relative to 5.6 mmol/l glucose as 100% (mean ± SE). *$P < 0.05$ vs. cells incubated with 5.6 mmol/l glucose ($n = 4$).

Immunohistochemistry. Moderately hyperglycemic diabetic mice and age-matched control mice were killed by anesthetization after 2 weeks. Kidneys were removed, and an immunohistochemical experiment was performed as described (21). Rabbit polyclonal anti-murine COX-2 antiserum (diluted 1:4,000; Cayman Chemical) was used for immunohistochemical detection of renal COX-2, and the same concentration of nonimmune rabbit IgG was used as a control. These were followed by counterstaining with hematoxylin (Sigma). Sections of each diabetic kidney were processed in parallel with appropriate control tissue.

Statistical analysis. Data were expressed as mean ± SE. Differences between two groups were evaluated by the unpaired Student's t test. $P < 0.05$ denoted the presence of a statistically significant difference.

RESULTS

Effects of high glucose on expression of COX-2 and COX-1 mRNA in HMCs. The mRNA levels of COX-1 and COX-2 were measured by the quantitative RT-PCR assay. As shown in Fig. 1, a significant increase of COX-2 mRNA was observed under 30 mmol/l glucose conditions compared with 5.6 mmol/l glucose (415.2 ± 35.8% of 5.6 mmol/l glucose), whereas COX-1 mRNA was unchanged under 30 mmol/l glucose. In addition, expression of COX-2 mRNA did not change after incubation with medium containing 5.6 mmol/l glucose plus 24.4 mmol/l mannitol, which was of equal osmotic pressure to 30 mmol/l glucose (data not shown).
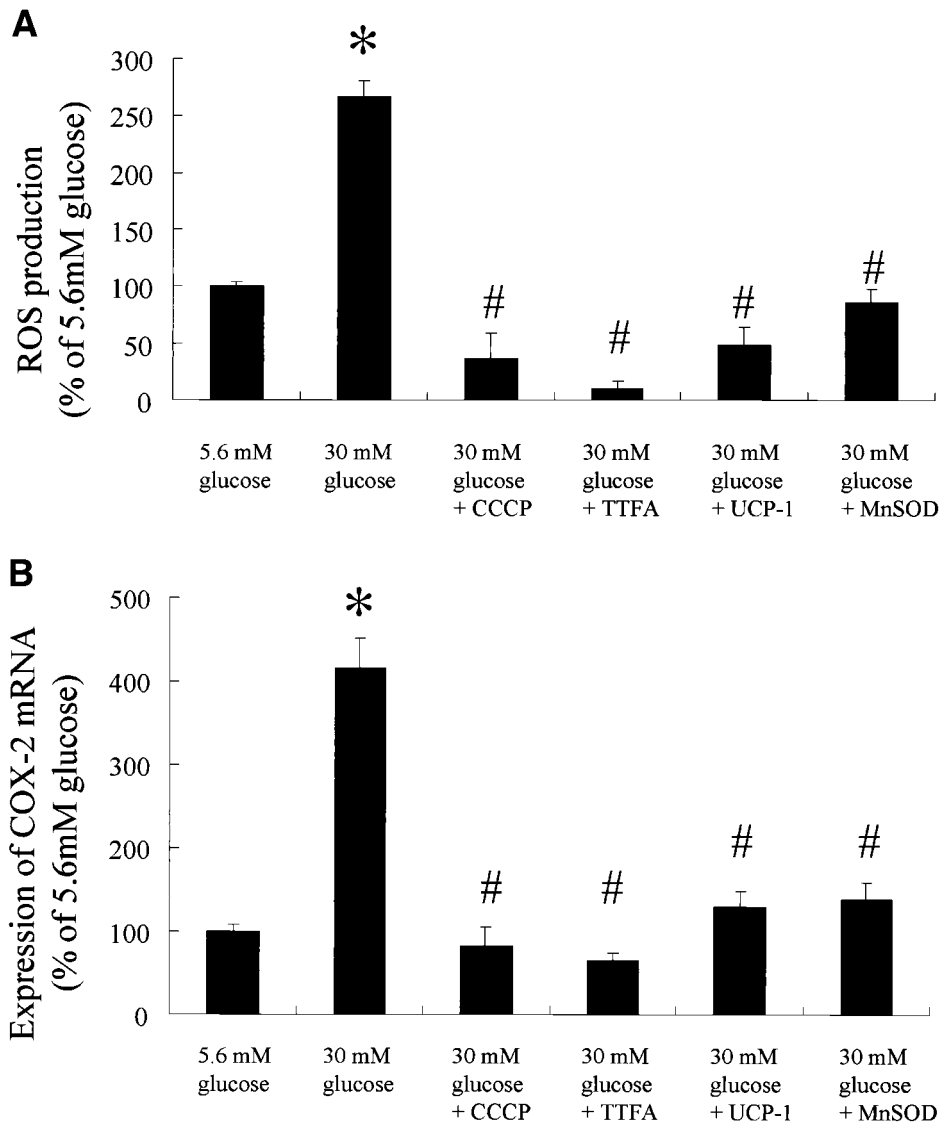
Effects of high glucose and agents that alter mito-chondrial metabolism on production of ROS in HMCs. To evaluate whether high glucose could increase redox changes in the mitochondria, we loaded cells with two fluorescence probes, MitoTracker Green FM and Redox-Sensor Red CC-1. As shown in Fig. 2, the fluorescence of MitoTracker Green FM (green fluorescence) stained for mitochondria. In contrast, RedoxSensor Red CC-1 (red fluorescence) staining seemed dependent on the cytosolic redox potential of each cell. An increase in yellow fluorescence induced by increased mitochondrial membrane potential was observed when the cells were incubated with 30 mmol/l glucose compared with 5.6 mmol/l glucose (Fig. 2, Merge). As shown in Fig. 3A, C-2938–associated fluorescence, representing intracellular ROS production, was significantly increased by incubation with 30 mmol/l glucose (290.5 ± 15.0% of 5 mmol/l glucose). In addition, this hyperglycemia-induced ROS overproduction was entirely

A 5.6 mM glucose

B 30 mM glucose
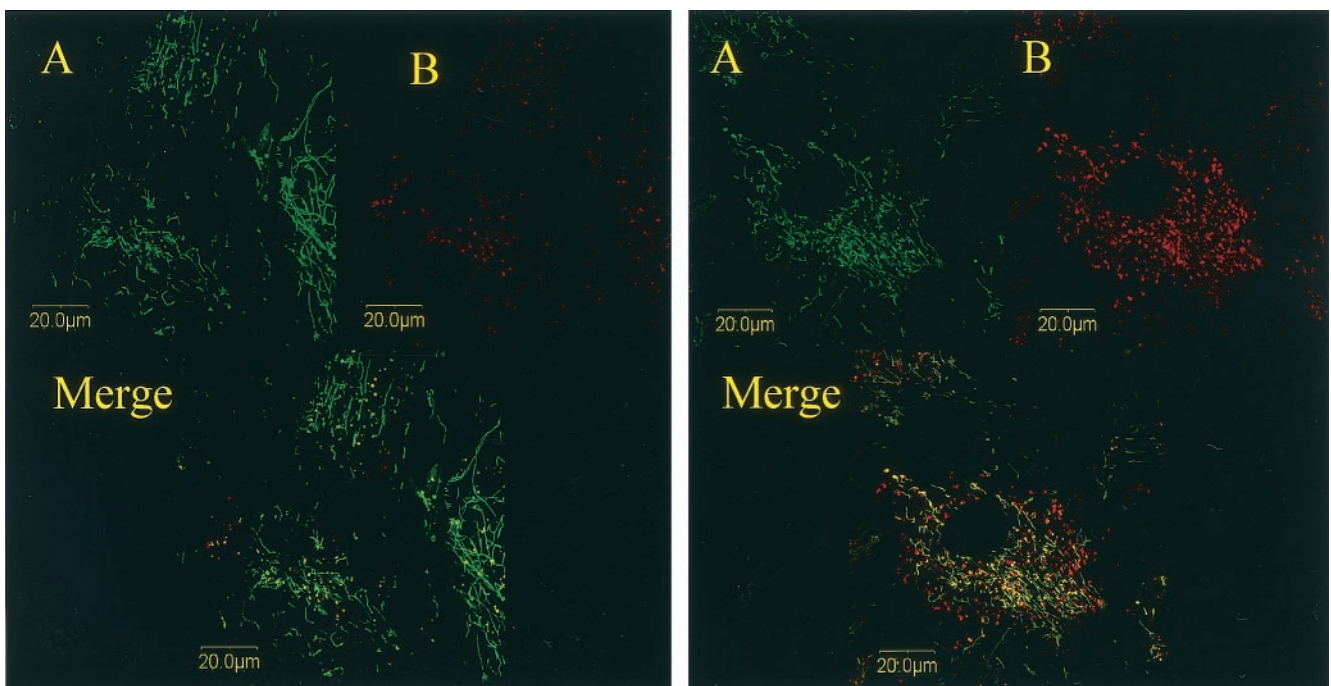
FIG. 2. Fluorescence and light microscopy examinations using MitoTracker Green FM and RedoxSensor Red CC-1. Cells were incubated in 5.6 mmol/l glucose (*left*) or 30 mmol/l glucose (*right*). After 3 h, cells were stained with MitoTracker Green FM (green; *A*), RedoxSensor Red CC-1 (red; *B*), and both (yellow; Merge). A confocal laser-scanning microscope was equipped for epifluorescent illumination. Scale bar = 20 μm.

A

B

FIG. 3. Effect of high glucose and agents that alter mitochondrial metabolism on ROS production and expression of COX-2 mRNA in HMCs. Cells were incubated with 5.6 mmol/l glucose, 30 mmol/l glucose, or 30 mmol/l glucose plus TTFA, CCCP, UCP-1, or MnSOD. *A*: ROS production was quantified using the fluorescent probe C-2938 ($n = 9$). *B*: Expression of COX-2 mRNA was quantified by a real-time RT-PCR method ($n = 4$). Results are expressed as values relative to 5.6 mmol/l glucose as 100% (mean ± SE). *$P < 0.05$ vs. cells incubated with 5.6 mmol/l glucose; #$P < 0.05$ vs. cells incubated with 30 mmol/l glucose.

suppressed by TTFA, an inhibitor of electron transport chain complex II, by CCCP, an uncoupler of oxidative phosphorylation, and by overexpression of either UCP-1 or MnSOD (37.7 ± 22, 11.1 ± 6.2, 47.9 ± 15.6, and 86.5 ± 10.8% of 5.6 mmol/l glucose, respectively).

Effects of agents that alter mitochondrial metabolism on induction of COX-2 mRNA in HMCs. We also assessed the effect of hyperglycemia-induced mitochondrial ROS overproduction on the induction of COX-2 mRNA by quantitative real-time RT-PCR. As shown in Fig. 3*B*, induction of COX-2 mRNA by 30 mmol/l glucose was suppressed by TTFA, CCCP, and overexpression of UCP-1 or MnSOD (66.0 ± 8.3, 82.0 ± 23.1, 129.9 ± 18.1, and 138.0 ± 21.1% of 5.6 mmol/l glucose, respectively).

Effects of high glucose and agents that alter mitochondrial metabolism on induction of COX-2 protein and PGE$_2$ synthesis in HMCs. Western blot analysis clearly demonstrated the induction of COX-2 protein in HMCs treated with 30 mmol/l glucose for 24 h (Fig. 4*A*). Similar to the results of ROS production and COX-2 mRNA expression, this effect was completely inhibited by overexpression of UCP-1 or MnSOD. As shown in Fig. 4*B*, production of PGE$_2$ from HMCs incubated with 30 mmol/l

glucose for 24 h was also significantly increased compared with that after incubation with 5.6 mmol/l glucose (151.1 ± 19.0 vs. 33.1 ± 4.0 pg · ml^{-1} · mg protein^{-1}, respectively) and completely inhibited in the presence of meloxicam, a relatively specific inhibitor of COX-2 (30.0 ± 2.5 pg · ml^{-1} · mg protein^{-1}). Inhibitors of mitochondrial metabolism, TTFA and CCCP (102 and 186% of 5 mmol/l glucose, respectively), as well as overexpression of UCP-1 or MnSOD (40.0 ± 5.7 and 48.1 ± 13.9 pg · ml^{-1} · mg protein^{-1}, respectively) induced similar decreases of PGE$_2$ synthesis. In addition, both the hyperglycemia-induced overproduction of PGE$_2$ and the normalizing effect on PGE$_2$ synthesis of the agents that altered mitochondrial metabolism were observed after a 72-h incubation with 30 mmol/l glucose (data not shown).

Functional promoter activity of the human COX-2 gene in HMCs. To determine whether the 5′-upstream region of the human COX-2 gene contains functional elements responsible for the hyperglycemia-induced upregulation of mRNA, we performed transient DNA transfection experiments using luciferase as a reporter gene in HMCs. The promoter activity with pGL3-pCOX2 (−497 to 32) was increased by 30 mmol/l glucose compared with 5.6
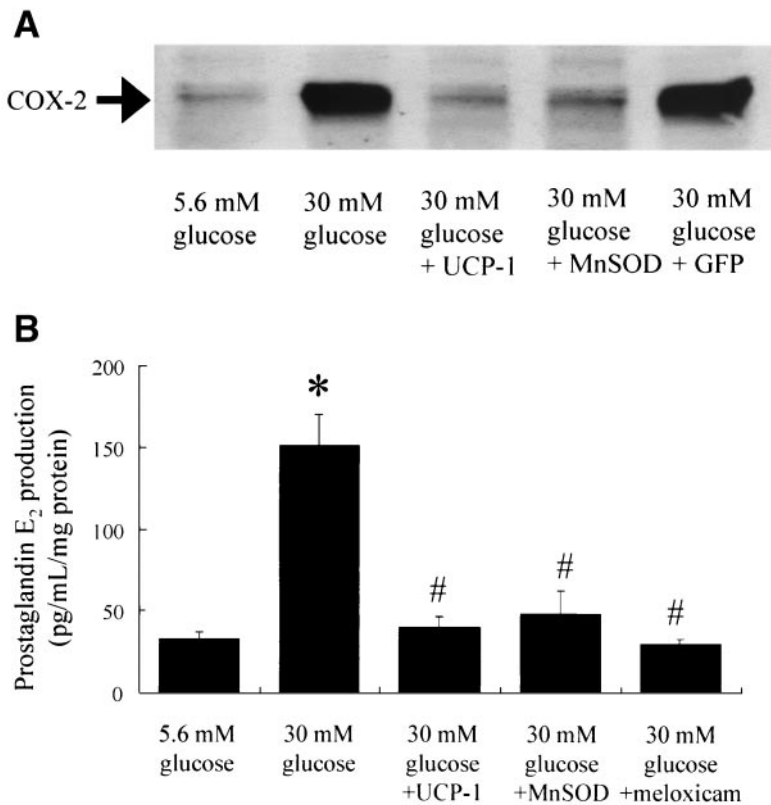
FIG. 4. Effect of high glucose and agents that alter mitochondrial metabolism on expression of COX-2 protein and PGE$_2$ production in HMCs. Cells were incubated with 5.6 mmol/l glucose, 30 mmol/l glucose, or 30 mmol/l glucose plus either UCP-1 or MnSOD for 24 h. A: Expression of COX-2 protein was evaluated by Western blot analysis. Similar results were obtained in two additional experiments. B: PGE$_2$ production in the media was measured using an enzyme immunosorbent assay kit. Results are expressed as values relative to 5.6 mmol/l glucose as 100% (mean ± SE). GFP, green fluorescent protein. *$P < 0.05$ vs. cells incubated with 5.6 mmol/l glucose; #$P < 0.05$ vs. cells incubated with 30 mmol/l glucose ($n = 4$).

mmol/l glucose (400.3 ± 34.8% of 5.6 mmol/l glucose; Fig. 5B). In addition, the induction was inhibited by overexpression of UCP-1 or MnSOD (131.7 ± 11.1 and 147.8 ± 16.1% of 5.6 mmol/l glucose, respectively). To evaluate the role of two consensus sequences for NF-κB binding sites that exist in the COX-2 promoter region, we performed site-directed mutagenesis of the NF-κB–5′ site (NF mut1), NF-κB–3′ site (NF mut2) (Fig. 5A), and both sites (NF mut1 and 2), and constructs bearing these mutations were transiently transfected into HMCs. A significant reduction in promoter activity was induced by mutation of each NF-κB site (NF mut1 and NF mut2: 235.8 ± 24.0 and 212.8 ± 4.8% of 5.6 mmol/l glucose with pGL3-pCOX2, respectively). Mutation of both NF-κB sites resulted in complete loss of hyperglycemia-induced activation of the promoter activity (NF mut1 and mut2: 46.5 ± 4.2% of 5.6 mmol/l glucose with pGL3-pCOX2) in the cells incubated with 30 mmol/l glucose. However, no significant effect of the mutations on promoter activity was observed in the cells incubated with 5.6 mmol/l glucose (Fig. 5C).

Expression of COX-2 mRNA and protein in glomeruli of control and streptozotocin-induced diabetic mice. To verify hyperglycemia-induced COX-2 expression in vivo, we measured expression of COX-2 mRNA and protein in glomeruli of control and streptozotocin-induced diabetic mice.

As shown in Fig. 6A, a significant increase of COX-2 mRNA measured by the quantitative RT-PCR assay was observed in glomeruli of diabetic mice compared with that of control mice (303.0 ± 53.0% of control). Similarly, Western blot analysis clearly demonstrated the increase of COX-2 protein in glomeruli of diabetic mice compared with that of control mice (Fig. 6B). In addition, an immunohistochemical staining against COX-2 protein was in-

creased in glomeruli of diabetic mice, including mesangial cells and podocytes, compared with that of control mice (Fig. 6C and D).

DISCUSSION

Production of ROS is increased in diabetic patients, especially in those with poor glycemic control (22). Oxidative damage may contribute to the development of diabetic microangiopathic and macroangiopathic complications. We proposed recently that hyperglycemia-induced ROS production from mitochondria is a key event in the development of diabetic complications (2). In this study, to clarify the impact of mitochondrial ROS production on diabetic nephropathy, we examined whether mitochondrial ROS increased expression of the COX-2 gene in HMCs, which are the target cells in diabetic nephropathy.

First, we demonstrated that RedoxSensor Red CC-1–associated fluorescence was increased by incubation with 30 mmol/l glucose compared with 5.6 mmol/l glucose in HMCs. Mitochondrial staining by RedoxSensor Red CC-1 was reported to be diminished by treatment with CCCP, which abolishes the mitochondrial membrane proton gradient, suggesting that RedoxSensor Red CC-1 is transported into the mitochondria as a result of mitochondrial membrane potential (23). Because electron flow through the mitochondrial electron transport chain resulted in increased mitochondrial membrane potential, the increased RedoxSensor Red CC-1–associated fluorescence induced by 30 mmol/l glucose indicated increased electron flow through the mitochondrial electron transport chain. In addition, we demonstrated that hyperglycemia could induce increased dichlorofluorescein-associated fluorescence, indicating that hyperglycemia induced intracellular
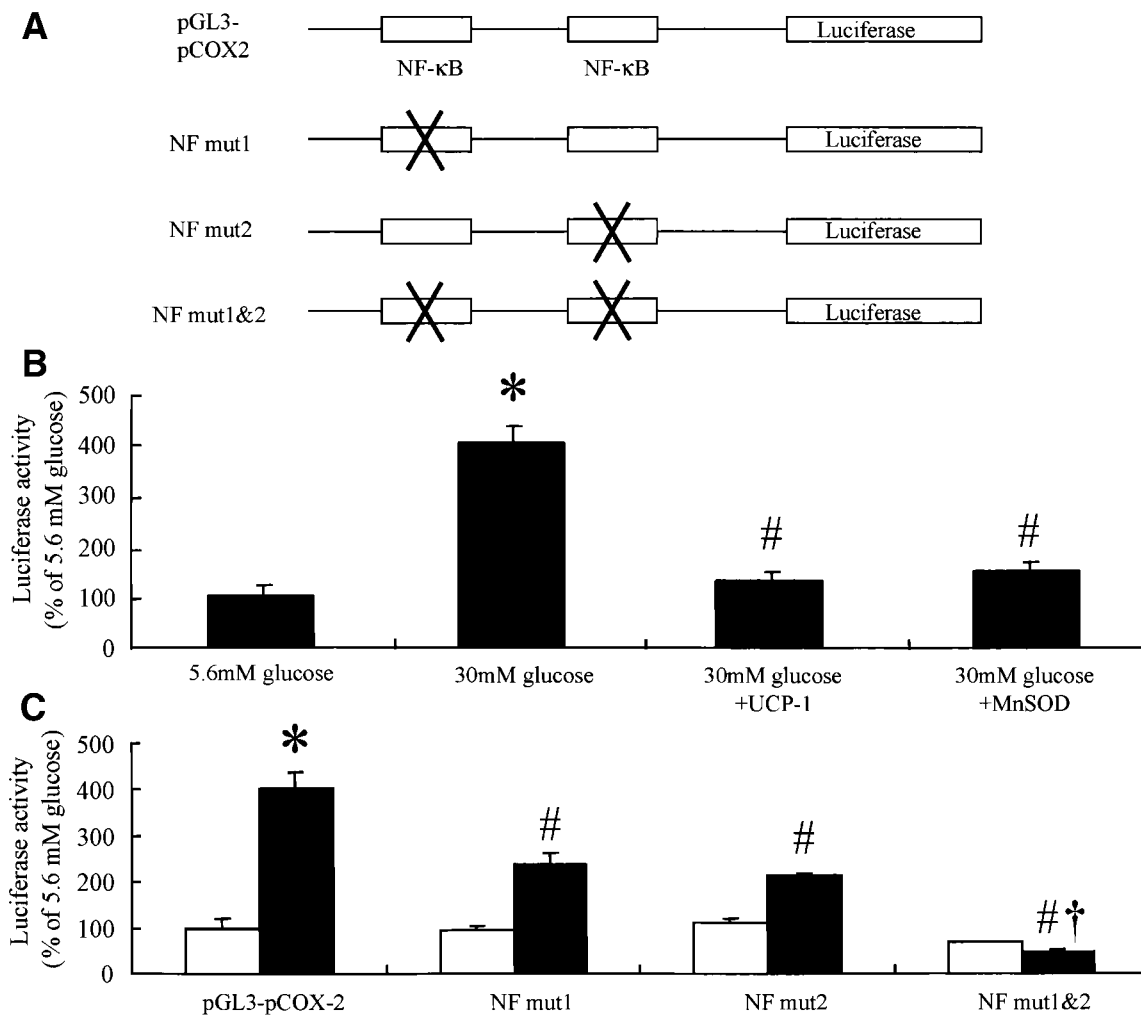
FIG. 5. Functional promoter activity of the human COX-2 gene in HMCs. *A*: A schematic diagram representing the wild-type pGL3-pCOX2 promoter and site-directed mutant constructs NF mut1, NF mut2, and NF mut1 and 2, used in transient transfection studies. Mutated sites are represented by crosses. *B*: Cells were transiently transfected with pGL3-pCOX2 and were incubated with 5.6 mmol/l glucose, 30 mmol/l glucose alone, or 30 mmol/l glucose plus either UCP-1 or MnSOD. *C*: Cells were transiently transfected with pGL3-pCOX2 or mutated vectors NF mut1, NF mut2, or NF mut1 and 2, and were incubated with 5.6 (□) or 30 (■) mmol/l glucose. Data are expressed relative to pGL3-pCOX2 of 5.6 mmol/l glucose and plotted as mean ± SE values. *$P < 0.05$ vs. pGL3-pCOX2–transfected cells incubated with 5.6 mmol/l glucose; #$P < 0.05$ vs. pGL3-pCOX2–transfected cells incubated with 30 mmol/l glucose; †$P < 0.05$ vs. NF mut1-transfected cells incubated with 30 mmol/l glucose ($n = 6$).

ROS production (2,18). This fluorescence was normalized by TTFA or CCCP or by overexpression of either UCP-1 or MnSOD in HMCs. This result suggests that hyperglycemia could increase ROS production through the mitochondrial electron transport chain in HMCs, which is similar to our previous observation in bovine endothelial cells.

Several investigators have demonstrated an increase in PG synthesis in glomerular and mesangial cells in experimental diabetes, and some studies have postulated a role for vasodilatory PGs in the glomerular hyperfiltration observed in early diabetes (3,4). A similar trend was observed in our results of hyperglycemia-induced PGE$_2$ synthesis in HMCs, as shown in Fig. 4*B*. Furthermore, we demonstrated that COX-2 mRNA and protein, an inducible and key enzyme of PG synthesis, were increased by 30 mmol/l glucose. To clarify that hyperglycemia-induced COX-2 expression was also observed in vivo, we used a new technique using spherical superparamagnetic beads to isolate glomeruli. This technique is fast and allows for the isolation of virtually all glomeruli present in a mouse

kidney at 97% purity (17). Consequently, we confirmed that both COX-2 mRNA and protein were increased in glomeruli of streptozotocin-induced diabetic mice. It is interesting that immunohistochemical staining localized COX-2 immunoreactivity in both mesangial cells and podocytes in glomeruli of diabetic mice, although the mechanism and role of COX-2 expression in podocytes is unclear. Further study will be required to elucidate the role of podocytes in the pathogenesis of diabetic nephropathy. Our results are in agreement with those of Komers et al. (21), who reported increased immunoreactivity for COX-2 in the renal cortex of streptozotocin-induced diabetic rats compared with control rats, which was normalized by treatment with insulin. In addition, the same group demonstrated that a selective inhibitor of COX-2 significantly decreased the glomerular filtration rate in diabetic rats (21). However, the mechanisms by which COX-2 is induced by hyperglycemia have not been clarified. We observed that both COX-2 induction and PGE$_2$ synthesis were normalized by an inhibitor of the electron transport
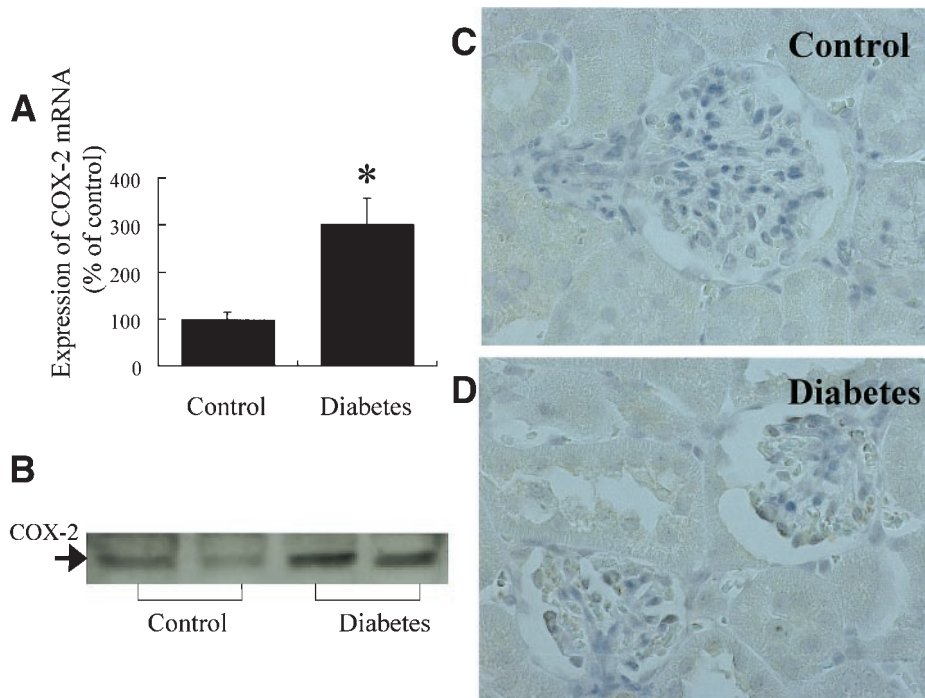
FIG. 6. Expression of COX-2 mRNA and protein in glomeruli of streptozotocin-induced diabetic mice. *A*: Glomeruli were isolated by using magnetic 4.5-μm-diameter Dynabeads. COX-2 mRNA was measured by the quantitative RT-PCR assay. Results are expressed as values relative to control mice as 100% (mean ± SE). *$*P < 0.05$ vs. control mice ($n = 3$). *B*: Glomeruli were isolated, and expression of COX-2 protein was evaluated by Western blot analysis. Similar results were obtained in two additional experiments. *C* and *D*: Kidneys were removed from control (*C*) and streptozotocin-induced diabetic mice (*D*). An immunohistochemical experiment was performed. Rabbit polyclonal anti-murine COX-2 antiserum was used for immunohistochemical detection of renal COX-2 and followed by counterstaining with hematoxylin. Magnification ×400.

chain complex II, by an uncoupler of oxidative phosphorylation, and by overexpression of UCP-1 or MnSOD, all of which could also normalize ROS production from the mitochondria. To the best of our knowledge, this is the first report to authenticate the association among mitochondrial ROS production and hyperglycemia, COX-2 induction, and PGE$_2$ synthesis in HMCs.

The human COX-2 gene maps to chromosome 1 (12) and contains a canonical TATA box 32 bp upstream and putative binding motifs for AP1, NF-κB, NF–interleukin (IL)-6 AP2, Sp1, and cAMP response element within the 497 bp upstream of the transcription start site (19). Given our findings in reporter gene transfection assays using MnSOD- or UCP-1–overexpressing cells, it seems that hyperglycemia increases COX-2 promoter activity, which is mediated by overproduction of mitochondrial ROS. In addition, wild-type/mutant constructs of reporter gene assays demonstrated that the two binding motifs for NF-κB located $-452/-442$ bp and $-228/-208$ bp upstream from the transcription start site of the COX-2 gene are important for hyperglycemia-induced COX-2 expression. Mutation of either one of the NF-κB binding sites had a partial inhibitory effect, whereas mutation of both sites resulted in complete inhibition, suggesting a synergistic effect of the two NF-κB sites on induction of the COX-2 gene by hyperglycemia. In agreement with these observations, we previously showed that hyperglycemia could activate NF-κB in bovine endothelial cells through overproduction of mitochondrial ROS (2). In addition, an NF-κB site located $-228/-208$ upstream from the transcription start site was reported to be important for the induction of COX-2 gene by both tumor necrosis factor-α (24) and hypoxia (25). In contrast, Allport et al. (20) reported that it is the cooperative interaction of proteins that bind to the AP-1 and -2 NF-κB sites that regulates IL-1β–stimulated COX-2 gene expression in epithelial cells. Furthermore, Inoue et al. (26) showed that the induction of COX-2 transcription by lipopolysaccharide

and phorbol ester involves the cAMP response element and NF–IL-6 sites in endothelial cells. COX-2 gene transcription induced by several agonists is likely to be mediated by multiple, complex signaling pathways leading to the binding of nuclear transcription activators to specific binding motifs. Further studies are required to clarify the role of other putative binding motifs in the activation of COX-2 gene by hyperglycemia.

The data reported here provide important implications for the design of new pharmacological approaches to prevent diabetic nephropathy. Although supplementation with α-tocopherol, a potent antioxidant, normalized retinal blood flow and creatinine clearance without changing HbA$_{1c}$ in patients with type 1 diabetes (27), low-dose vitamin E failed to alter the risk of cardiovascular and renal diseases in patients with diabetes (28). Blocking hyperglycemia-induced mitochondrial ROS production by new pharmacological agents could offer an additional strategy for the potential prevention of diabetic nephropathy. Two novel low-molecular mass compounds, M40403 (29) and EUK-134 (30), were developed as functional mimics of SOD enzymes. Such compounds have high catalytic SOD activity. In addition, injection of M40403 into rat models of inflammation and ischemia-reperfusion injury protected the animals against tissue damage, and treatment of adult hermaphrodite worms with EUK-134 caused a large increase in lifespan (30). Further studies in vivo in experimental animals will be required to confirm the impact of mitochondrial ROS production on progression of diabetic nephropathy.

In conclusion, our study has demonstrated that hyperglycemia increases ROS production through the mitochondrial electron transport chain. This ROS production results in activation of NF-κB, induction of COX-2 mRNA and protein through an increase in its promoter activity, and finally induction of PGE$_2$ synthesis in HMCs. These results suggest that ROS play a central role in the pathogenesis of the glomerular hyperfiltration observed in early diabetes,

and this integrating paradigm could provide a new conceptual framework for future research and therapy for diabetic nephropathy.

REFERENCES

1. Baynes JW: Role of oxidative stress in development of complications in diabetes. *Diabetes* 40:405–412, 1991
2. Nishikawa T, Edelstein D, Du XL, Yamagishi S, Matsumura T, Kaneda Y, Yorek MA, Beebe D, Oates PJ, Hammes HP, Giardino I, Brownlee M: Normalizing mitochondrial superoxide production blocks three pathways of hyperglycaemic damage. *Nature* 404:787–790, 2000
3. Ditzel J, Schwartz M: Abnormally increased glomerular filtration rate in short-term insulin-treated diabetic subjects. *Diabetes* 16:264–267, 1967
4. Hostetter TH, Troy JL, Brenner BM: Glomerular hemodynamics in experimental diabetes mellitus. *Kidney Int* 19:410–415, 1981
5. Arima S, Ren Y, Juncos LA, Carretero OA, Ito S: Glomerular prostaglandins modulate vascular reactivity of the downstream efferent arterioles. *Kidney Int* 45:650–658, 1994
6. Schambelan M, Blake S, Sraer J, Bens M, Nivez MP, Wahbe F: Increased prostaglandin production by glomeruli isolated from rats with streptozotocin-induced diabetes mellitus. *J Clin Invest* 75:404–412, 1985
7. Craven PA, Caines MA, DeRubertis FR: Sequential alterations in glomerular prostaglandin and thromboxane synthesis in diabetic rats: relationship to the hyperfiltration of early diabetes. *Metabolism* 36:95–103, 1987
8. Wu KK: Cyclooxygenase 2 induction: molecular mechanism and pathophysiologic roles. *J Lab Clin Med* 128:242–245, 1996
9. Sirois J, Richards JS: Purification and characterization of a novel, distinct isoform of prostaglandin endoperoxide synthase induced by human chorionic gonadotropin in granulosa cells of rat preovulatory follicles. *J Biol Chem* 267:6382–6388, 1992
10. Tetsuka T, Daphna-Iken D, Miller BW, Guan Z, Baier LD, Morrison AR: Nitric oxide amplifies interleukin 1-induced cyclooxygenase-2 expression in rat mesangial cells. *J Clin Invest* 97:2051–2056, 1996
11. Harris RC, McKanna JA, Akai Y, Jacobson HR, Dubois RN, Breyer MD: Cyclooxygenase-2 is associated with the macula densa of rat kidney and increases with salt restriction. *J Clin Invest* 94:2504–2510, 1994
12. Tazawa R, Xu XM, Wu KK, Wang LH: Characterization of the genomic structure, chromosomal location and promoter of human prostaglandin H synthase-2 gene. *Biochem Biophys Res Commun* 203:190–199, 1994
13. Ichihara A, Imig JD, Inscho EW, Navar LG: Cyclooxygenase-2 participates in tubular flow-dependent afferent arteriolar tone: interaction with neuronal NOS. *Am J Physiol* 275:F605–F612, 1998
14. Oh JH, Ha H, Yu MR, Lee HB: Sequential effects of high glucose on mesangial cell transforming growth factor-beta 1 and fibronectin synthesis. *Kidney Int* 54:1872–1878, 1998
15. Du XL, Edelstein D, Rossetti L, Fantus IG, Goldberg H, Ziyadeh F, Wu J, Brownlee M: Hyperglycemia-induced mitochondrial superoxide overproduction activates the hexosamine pathway and induces plasminogen activator inhibitor-1 expression by increasing Sp1 glycosylation. *Proc Natl Acad Sci U S A* 97:12222–12226, 2000
16. Bendriss-Vermare N, Barthelemy C, Durand I, Bruand C, Dezutter-Dambuyant C, Moulian N, Berrih-Aknin S, Caux C, Trinchieri G, Briere F: Human thymus contains IFN-alpha-producing CD11c(-), myeloid CD11c(+), and mature interdigitating dendritic cells. *J Clin Invest* 107:835–844, 2001
17. Takemoto M, Asker N, Gerhardt H, Lundkvist A, Johansson BR, Saito Y, Betsholtz C: A new method for large scale isolation of kidney glomeruli from mice. *Am J Pathol* 161:799–805, 2002
18. Wang H, Joseph JA: Quantifying cellular oxidative stress by dichlorofluorescein assay using microplate reader. *Free Radic Biol Med* 27:612–616, 1999
19. Lukiw WJ, Pelaez RP, Martinez J, Bazan NG: Budesonide epimer R or dexamethasone selectively inhibit platelet-activating factor-induced or interleukin 1beta-induced DNA binding activity of cis-acting transcription factors and cyclooxygenase-2 gene expression in human epidermal keratinocytes. *Proc Natl Acad Sci U S A* 95:3914–3919, 1998
20. Allport VC, Slater DM, Newton R, Bennett PR: NF-κB and AP-1 are required for cyclo-oxygenase 2 gene expression in amnion epithelial cell line (WISH). *Mol Hum Reprod* 6:561–565, 2000
21. Komers R, Lindsley JN, Oyama TT, Schutzer WE, Reed JF, Mader SL, Anderson S: Immunohistochemical and functional correlations of renal cyclooxygenase-2 in experimental diabetes. *J Clin Invest* 107:889–898, 2001
22. Giugliano D, Ceriello A, Paolisso G: Oxidative stress and diabetic vascular complications. *Diabetes Care* 19:257–267, 1996
23. Chen CS, Gee KR: Redox-dependent trafficking of 2,3,4,5, 6-pentafluorodihydrotetramethylrosamine, a novel fluorogenic indicator of cellular oxidative activity. *Free Radic Biol Med* 28:1266–1278, 2000
24. Yamamoto K, Arakawa T, Ueda N, Yamamoto S: Transcriptional roles of nuclear factor kappa B and nuclear factor-interleukin-6 in the tumor necrosis factor alpha-dependent induction of cyclooxygenase-2 in MC3T3–E1 cells. *J Biol Chem* 270:31315–31320, 1995
25. Schmedtje JF Jr, Ji YS, Liu WL, DuBois RN, Runge MS: Hypoxia induces cyclooxygenase-2 via the NF-κB p65 transcription factor in human vascular endothelial cells. *J Biol Chem* 272:601–608, 1997
26. Inoue H, Yokoyama C, Hara S, Tone Y, Tanabe T: Transcriptional regulation of human prostaglandin-endoperoxide synthase-2 gene by lipopolysaccharide and phorbol ester in vascular endothelial cells: involvement of both nuclear factor for interleukin-6 expression site and cAMP response element. *J Biol Chem* 270:24965–24971, 1995
27. Bursell SE, Clermont AC, Aiello LP, Aiello LM, Schlossman DK, Feener EP, Laffel L, King GL: High-dose vitamin E supplementation normalizes retinal blood flow and creatinine clearance in patients with type 1 diabetes. *Diabetes Care* 22:1245–1251, 1999
28. Heart Outcomes Prevention Evaluation Study Investigators: Effects of ramipril on cardiovascular and microvascular outcomes in people with diabetes mellitus: results of the HOPE study and MICRO-HOPE substudy. *Lancet* 355:253–259, 2000
29. Salvemini D, Wang ZQ, Zweier JL, Samouilov A, Macarthur H, Misko TP, Currie MG, Cuzzocrea S, Sikorski JA, Riley DP: A nonpeptidyl mimic of superoxide dismutase with therapeutic activity in rats. *Science* 286:304–306, 1999
30. Melov S, Ravenscroft J, Malik S, Gill MS, Walker DW, Clayton PE, Wallace DC, Malfroy B, Doctrow SR, Lithgow GJ: Extension of life-span with superoxide dismutase/catalase mimetics. *Science* 289:1567–1569, 2000